Inorganic Chemistry

ARTICLE

pubs.acs.org/IC

Cation−Cation Interactions: Crystal Structures of Neptunyl(V) Selenate Hydrates, $(NpO_2)_2(SeO_4)(H_2O)_n$ (n = 1, 2, and 4)

Geng Bang Jin, S. Skanthakumar, and L. Soderholm*

Chemical Sciences and Engineering Division, Argonne National Laboratory, Argonne, Illinois 60439, United States

Supporting Information

ABSTRACT: Green crystals of $(NpO_2)_2(SeO_4)(H_2O)_4$, $(NpO_2)_2(SeO_4)(H_2O)_2$, and $(NpO_2)_2(SeO_4)(H_2O)$ have been prepared by hydrothermal methods. The structures of these compounds have been characterized by single-crystal X-ray diffraction. $(NpO_2)_2(SeO_4)(H_2O)_4$, isostructural with $(NpO_2)_2(SO_4)(H_2O)_4$, is constructed from layers comprised of corner-sharing neptunyl(V) pentagonal bipyramids and selenate tetrahedra that are further linked by hydrogen bonding with water molecules. Each NpO_2^+ cation binds to four other NpO_2^+ units through cation−cation interactions (CCIs) to form a distorted "cationic square net" decorated by SeO_4^{2-} tetrahedra above and below the layer. Each selenate anion is bound to two neptunyl(V) cations through monodentate linkages. $(NpO_2)_2(SeO_4)(H_2O)_2$ is isostructural with the corresponding sulfate analogue as well. It consists of puckered layers of neptunyl(V) pentagonal bipyramids that are further connected by selenate tetrahedra to form a three-dimensional framework. The CCI pattern in the neptunyl layers of dihydrate is very similar to that of tetrahydrate; however, each SeO_4^{2-} tetrahedron is bound to four NpO_2^+ cations in a mondentate manner. $(NpO_2)_2(SeO_4)(H_2O)$ crystallizes in the monoclinic space group $P2_1/c$, which differs from the $(NpO_2)_2(SO_4)(H_2O)$ orthorhombic structure due to the slightly different connectivities between NpO_2^+ cations and anionic ligands. The structure of $(NpO_2)_2(SeO_4)(H_2O)$ adopts a three-dimensional network of distort neptunyl(V) pentagonal bipyramids decorated by selenate tetrahedra. Each NpO_2^+ cation connects to four other NpO_2^+ units through CCIs and also shares an equatorial coordinating oxygen atom with one of the other units in addition to the CC bond to form a dimer. Each SeO_4^{2-} tetrahedron is bound to five NpO_2^+ cations in a monodentate manner. Magnetic measurements obtained from the powdered tetrahydrate are consistent with a ferromagnetic ordering of the neptunyl(V) spins at 8(1) K, with an average low temperature saturation moment of 1.98(8) μ_B per Np. Well above the ordering temperature, the susceptibility follows Curie−Weiss behavior, with an average effective moment of 3.4(2) μ_B per Np and a Weiss constant of 14(4) K. Correlations between lattice dimensionality and magnetic behavior are discussed.

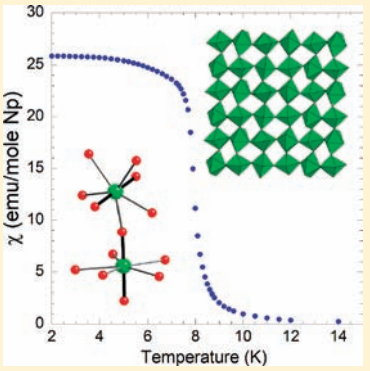

INTRODUCTION

Neptunium (Np) is the first in the series of manmade, transuranic elements, comprising radioisotopes with atomic numbers greater than 92.[1] Somewhat similar in chemistry to uranium,[2] Np may exist in the tri- to heptavalent oxidation states, although its aquatic chemistry is dominated by the pentavalent cation Np(V), which typically exists as the linear dioxo cation, NpO_2^+.[1] A byproduct of the ^{235}U fuel cycle, it is considered one of the most problematic actinides for long-term nuclear-waste storage due to the long half-life of the ^{237}Np isotope (2.14×10^6 years).[3−5] Exacerbating the situation is the relatively weak complexing ability of the monovalent cation NpO_2^+ and the high solubility of its solids, which taken together render neptunyl(V) very mobile in the environment.[4−6] Consistent with other actinyl cations, NpO_2^+ completes its coordination environment with four to six ligands coordinating equatorial to the dioxo moeity.[7,8] In contrast to the uranyl(VI) and neptunyl-(VI) cations, neptunyl(V) dioxo ions have a tendency to bond to other NpO_2^+ units as an equatorial ligand. This bonding between NpO_2^+ cations via the neptunyl oxygen was first observed in solution, which was referred to as a cation−cation interaction (CCI).[9] Since that time, neptunyl(V) CCIs have been widely observed in solution, where they affect the speciation and redox chemistry,[10−12] and in the solid state, where they influence structural motifs as well as electronic and magnetic properties.[8,13] Notably, CCIs between NpO_2^+ units impart the potential for tunable lattice dimensionality together with super-exchange pathways that can enhance magnetic interactions between neighboring Np(V) ($5f^2$) ions.[14] To our knowledge, all neptunyl(V) compounds reported to date that exhibit magnetic ordering include CCIs.[14−21] The structural diversity, coupled with the similar electronic properties expected for an f^2 system in a strong axial field, make neptunyl(V) compounds an interesting avenue into studies relating lattice and spin dimensionality in localized f-electron compounds.

Of some relevance due to their environmental and technological importance, numerous Np(V) compounds containing tetrahedral oxo anions of the hexavalent group VI elements (S, Se, Cr, and Mo) have been structurally characterized.[8,22,23] Structural studies of

Received: March 10, 2011
Published: April 26, 2011

neptunyl(V) sulfates are particular interesting, as all reported compounds with Np:S ratio ≥1:1 contain CCIs.[15,24−29] Examples include $(NpO_2)_2(SO_4)(H_2O)_n$ (n = 1, 2, 4, 6),[24−28] $NaK_3(NpO_2)_4(SO_4)_4(H_2O)_2$,[15] and $Na(NpO_2)(SO_4)(H_2O)$.[15] The CCI networks reported for these compounds include one-dimensional NpO_2^+ chains and ribbons, two-dimensional sheets, and a condensed three-dimensional structure.[8,13] Only magnetic properties of $NaK_3(NpO_2)_4(SO_4)_4(H_2O)_2$ and $Na(NpO_2)(SO_4)(H_2O)$ have been reported, both of which undergo ferromagnetic ordering, at 6.5(5) and 7.4(1) K, respectively.[15]

With the goal of characterizing the magnetic properties of related materials, efforts were undertaken to synthesize some neptunyl(V) selenates, although it is unclear to what extent a close correspondence is expected with the sulfate structures. Looking to uranyl(VI) chemistry, a divergence is seen in the UO_2^{2+}−sulfate and −selenate interactions. For the most part, uranyl sulfates have the typical two-dimensional sheet structures exhibited by the uranyl ion,[7] whereas the selenates are known to crystallize in novel, nanoscale tubules.[30,31] High energy X-ray scattering (HEXS) studies on UO_2^{2+}−sulfate and −selenate ion pairs show this behavior to persist in solution. Instead of rotating about the U−O−S bond, the uranyl to sulfate-ion orientation appears rigid in aqueous solution,[32] in contrast to uranyl selenate ion pairs, which appear to rotate freely,[33] suggesting an inherent electrostatic origin to the structural differences. The results of similar studies for neptunyl(V) solutions were compromised by the presence of CCIs.[12]

In the solid state, few neptunyl(V) selenates have been structurally characterized, providing little precedent. $(NpO_2)_2(SeO_4)(H_2O)_n$ (n = 1, 2, 4, 6)[25] compounds are reported and have been considered isostructural with the sulfate analogues, although no crystallographic information has been provided. Their electronic absorption spectra are identical to those of the corresponding sulfates, indicating the presence of similar CCI structures.[25] The structure of $Co(NH_3)_6NpO_2(SeO_4)_2(H_2O)_3$[34] has been reported and consists of $[NpO_2(SeO_4)_2(H_2O)]^{3-}$ layers without direct interactions between NpO_2^+ ions, but the sulfate analogue has not been reported. With little structural precedent, it is worthwhile to explore the neptunyl(V) selenate chemistry and to reinvestigate known phases, especially those with high metal:ligand ratios. Further insight is sought into CCIs and how they affect the crystal chemistry of neptunyl(V) compounds, with the goal of expanding examples of the interplay between lattice and spin dimensionality in 5f systems. Herein, we present the syntheses and single-crystal structures of $(NpO_2)_2(SeO_4)(H_2O)_4$, $(NpO_2)_2(SeO_4)(H_2O)_2$, and $(NpO_2)_2(SeO_4)(H_2O)$ and report the magnetic property of $(NpO_2)_2(SeO_4)(H_2O)_4$.

EXPERIMENTAL SECTION

Caution! *^{237}Np is an α- and γ-emitting radioisotope and as such is considered a health risk. Its use requires appropriate infrastructure and personnel trained in the handling of radioactive materials.*

Hydrothemal Syntheses[35] of $(NpO_2)_2(SeO_4)(H_2O)_n$ (n = 1, 2, 4). 38.5 mg (0.104 mmol) of $Na_2SeO_4\cdot 10H_2O$ (Aldrich, 99.999%) and 0.025 mL of 2 M NaOH (Fisher, 98.5%) were added to 0.15 mL of a 0.167 M solution of NpO_2^+ in 0.86 M HCl. The resulting mixture was loaded into a 3 mL Teflon cup with a tightly closed screw-top lid. Two Teflon cups were placed in a 125 mL Teflon-lined Parr reaction vessel with 30 mL counter-pressure water and heated in a convection oven at 150 °C for 6 days, and then the oven was turned off. The major reaction product is pale green rectangular plates of $(NpO_2)_2(SeO_4)(H_2O)_4$. Two bright green polyhedral crystals of $(NpO_2)_2(SeO_4)(H_2O)_2$ (0.1−0.2 mm in length) and one dark green polyhedral crystal of $(NpO_2)_2(SeO_4)(H_2O)$ (∼0.15 mm in length) were also found in the same reaction, which were manually separated from the tetrahydrate crystals. On the basis of this visual sorting method, we estimate yields of more than 99% for the tetrahydrate and less than 1% for the other two phases. Powder X-ray diffraction measurements confirmed the phase purity of $(NpO_2)_2(SeO_4)(H_2O)_4$ by comparison with powder patterns calculated from the single-crystal X-ray structures.

Structure Determinations. Single-crystal X-ray diffraction data for $(NpO_2)_2(SeO_4)(H_2O)_4$, $(NpO_2)_2(SeO_4)(H_2O)_2$, and $(NpO_2)_2(SeO_4)(H_2O)$ were collected with the use of graphite-monochromatized Mo Kα radiation (λ = 0.71073 Å) at 100 K on a Bruker APEX2 diffractometer.[36] The crystal-to-detector distance was 5.106 cm. Data for $(NpO_2)_2(SeO_4)(H_2O)_4$ were collected by a scan of 0.5° in ω in groups of 250 frames at φ settings of 0°, 90°, 180°, and 270° and 0.5° in φ in groups of 720 frames at ω settings of −28° and 210°. Data for $(NpO_2)_2(SeO_4)(H_2O)_2$ and $(NpO_2)_2(SeO_4)(H_2O)$ were collected by a scan of 0.3° in ω in groups of 600 frames at φ settings of 0°, 90°, 180°, and 270°. The exposure time was 25 s/frame for $(NpO_2)_2(SeO_4)(H_2O)_4$ and 20 s/frame for $(NpO_2)_2(SeO_4)(H_2O)_2$ and $(NpO_2)_2(SeO_4)(H_2O)$. The collection of intensity data as well as cell refinement and data reduction were carried out with the use of the program APEX2.[36] Absorption corrections for $(NpO_2)_2(SeO_4)(H_2O)_4$ (face indexed), $(NpO_2)_2(SeO_4)(H_2O)_2$, and $(NpO_2)_2(SeO_4)(H_2O)$, as well as incident beam and decay corrections were performed with the use of the program SADABS.[37] The structures were solved with the direct-methods program SHELXS and refined with the least-squares program SHELXL.[38] Each final refinement included anisotropic displacement parameters for all non-hydrogen atoms.

In the structural refinements of $(NpO_2)_2(SeO_4)(H_2O)_4$, only the two H atoms for water O(2) atom were located in the difference maps. H positions were refined using O−H and H−H distance constraints of 0.83 and 1.40 Å, respectively. Also, in the structural refinements of $(NpO_2)_2(SeO_4)(H_2O)_2$, only the two H atoms for water O(3) atom were located in the difference maps.The structure of $(NpO_2)_2(SeO_4)(H_2O)$ was successfully solved in the monoclinic space group $P2_1/c$ with R_1 index of 0.0260. The assignment of Np, Se, and O atoms was straightforward based on their electron densities and interatomic distances and angles. H atoms could not be identified from the difference Fourier maps, so they were not included in the structural refinements. The cell parameters of $(NpO_2)_2(SeO_4)(H_2O)$ (see Table 1) are comparable to those of $(NpO_2)_2(SO_4)(H_2O)$ (orthorhombic cell: a = 15.790(4), b = 6.932(2), and c = 6.714(2) Å; space group $Pnma$),[26] highlighting their structural similarities. Attempts to solve the structure of $(NpO_2)_2(SeO_4)(H_2O)$ using the model of $(NpO_2)_2(SO_4)(H_2O)$ in a orthorhombic cell (a = 15.679(7), b = 6.947(3), and c = 6.941(3) Å) failed. For example, the structure refinements of $(NpO_2)_2(SeO_4)(H_2O)$ with the space group $Pnma$ result in 110 systematic absence violations including a number of intense reflections and all non positive definite O atoms, clearly suggesting a different structural solution of $(NpO_2)_2(SeO_4)(H_2O)$ from $(NpO_2)_2(SO_4)(H_2O)$.

The program STRUCTURE TIDY[39] was used to standardize the positional parameters. Additional experimental details are given in Table 1 and in the Supporting Information.

Powder X-ray Diffraction Measurements. Powder X-ray diffraction patterns were collected with a Scintag X1 diffractometer with the use of Cu Kα radiation (λ = 1.5418 Å).

Magnetic Susceptibility Measurements. A superconducting quantum interference device (SQUID) magnetometer was used to measure the magnetic response of 3.8 mg crushed single crystals of $(NpO_2)_2(SeO_4)(H_2O)_4$ over the temperature range of 5 to 320 K. Because of the radiological hazards associated with ^{237}Np, the sample was double-encapsulated in a sealed aluminum holder that contributed considerably (up to 90% at high temperatures) to the measured response. Low temperature hysteresis measurements were obtained at 2, 5, 10, and 20 K as a function of field to a maximum of 4 T.

Table 1. Crystal Data and Structure Refinements for $(NpO_2)_2(SeO_4)(H_2O)_4$, $(NpO_2)_2(SeO_4)(H_2O)_2$, and $(NpO_2)_2(SeO_4)(H_2O)$[a]

	$(NpO_2)_2(SeO_4)(H_2O)_4$	$(NpO_2)_2(SeO_4)(H_2O)_2$	$(NpO_2)_2(SeO_4)(H_2O)$
fw	753.02	716.99	698.98
color and habit	pale green plate	bright green polyhedron	dark green polyhedron
crystal system	triclinic	monoclinic	monoclinic
space group	*P*-1	$P2_1/c$	$P2_1/c$
a (Å)	8.1672(8)	10.645(1)	6.9535(6)
b (Å)	16.229(2)	5.7609(6)	6.9406(6)
c (Å)	8.8478(9)	13.575(1)	15.683(1)
α (deg)	89.673(2)		
β (deg)	67.518(1)	97.903(1)	90.854(1)
γ (deg)	87.353(2)		
V (Å^3)	1082.4(2)	824.6(1)	756.8(1)
ρ_c (g/cm^3)	4.621	5.775	6.135
μ (cm^{-1})	225.08	295.12	321.38
$R(F)$[b]	0.0262	0.0253	0.0260
$R_w(F_o^2)$[c]	0.0541	0.0534	0.0541

[a] For all structures, $Z = 4$, $\lambda = 0.71073$ Å, and $T = 100(2)$ K. [b] $R(F) = \Sigma||F_o| - |F_c||/\Sigma|F_o|$ for $F_o^2 > 2\sigma(F_o^2)$. [c] $R_w(F_o^2) = \{\Sigma[w(F_o^2 - F_c^2)^2]/\Sigma wF_o^4\}^{1/2}$.

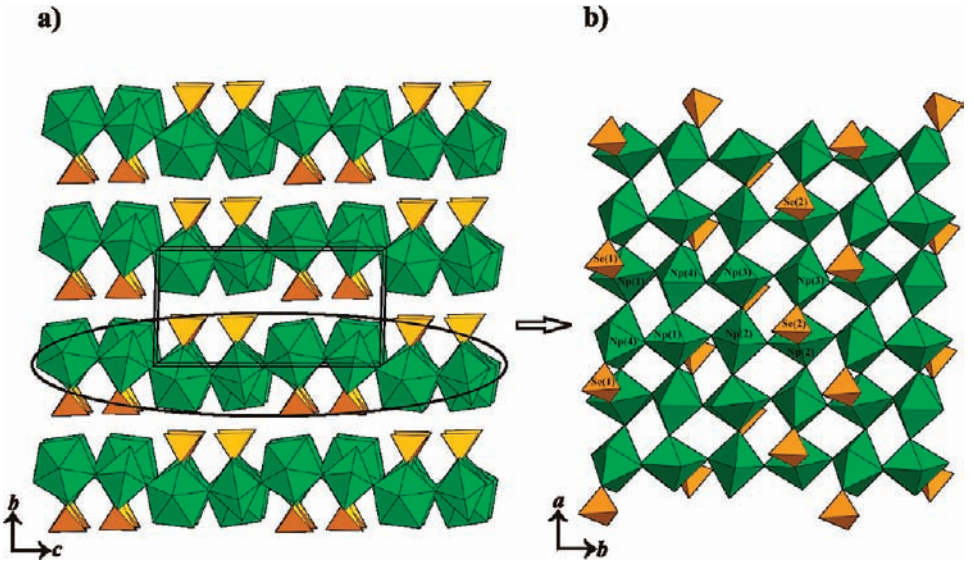

Figure 1. (a) Structure of $(NpO_2)_2(SeO_4)(H_2O)_4$ constructed by neptunyl and selenate polydedral layers (circled) that further connected by hydrogen bonding. (b) A depiction of an individual layer of corner-sharing green NpO_7 pentagonal bipyramids coordinated by orange SeO_4 tetrahedra.

Magnetization data as a function of temperature were acquired under applied fields of 0.005, 0.01, 0.05, 0.2, 0.5, and 1.0 T. Empty Al sample holders were measured separately under identical conditions, and their magnetic response was subtracted directly from the raw data. The measured susceptibility data were further corrected by removing the Langevin diamagnetic contribution of the sample from the raw data.[40,41] Insufficient quantities of the other two new materials, $(NpO_2)_2(SeO_4)(H_2O)_2$ and $(NpO_2)_2(SeO_4)(H_2O)$, were available to characterize their magnetic response.

RESULTS

Syntheses. Hydrothermal syntheses of $(NpO_2)_2(SeO_4)(H_2O)_n$ (n = 1, 2, 4) from the reactions of Np(V) and H_2SeO_4 solutions have been mentioned by Bessonov et al.;[25] however, no further experimental details were reported. We first prepared $(NpO_2)_2(SeO_4)(H_2O)_4$ in a high yield via a reaction of NpO_2^+ and $Na_2SeO_4 \cdot 10H_2O$. The synthesis also yielded a few crystals of $(NpO_2)_2(SeO_4)(H_2O)_2$ and $(NpO_2)_2(SeO_4)(H_2O)$. It is not uncommon to produce a mixture of neptunyl(V) crystals with different amount of hydrates. Similar behavior has been seen in neptunyl(V) sulfate and formate systems.[25,42] To prepare pure $(NpO_2)_2(SeO_4)(H_2O)_2$ and $(NpO_2)_2(SeO_4)(H_2O)$ phases, numerous reactions have been attempted with different synthetic parameters such as various concentrations and ratios of starting materials. Unfortunately, none of them were successful especially for the monohydrate. For example, reducing the amount of $Na_2SeO_4 \cdot 10H_2O$ in titled synthesis to 21.2 mg (0.057 mmol) resulted in about 5% $(NpO_2)_2(SeO_4)(H_2O)_2$, based on precipitate quantities, up from less than 1% in the original synthesis.

Structures. The structure of $(NpO_2)_2(SeO_4)(H_2O)_4$, shown in Figure 1a, is isotypic to $(NpO_2)_2(SO_4)(H_2O)_4$.[28] It consists of

dx.doi.org/10.1021/ic200479m |*Inorg. Chem.* 2011, 50, 5203–5214

layers of neptunyl pentagonal bipyramids and selenate tetrahedra in the *ab* plane, which are linked along the *c* axis only by hydrogen bonding with water ligands. Within the neptunyl selenate layers, each neptunyl polyhedron shares corners with four other units and one selenate tetrahedron, and connects to two water molecules (Figure 1b). There are four crystallographically unique Np, two Se, and 24 O positions. The local coordination environments for the Np atoms are all very similar, with each forming a nearly linear dioxo, neptunyl cation NpO_2^+. The Np−O distances within the NpO_2^+ unit range from 1.834(4) to 1.852(4) Å, and O−Np−O angles range from 178.1(2)° to 179.9(2)° (Table 2). Each NpO_2^+ cation is coordinated by two other NpO_2^+ units, one monodentate SeO_4^{2-} tetrahedron, and two water molecules in the equatorial plane to form a pentagonal bipyramid. For example, each $Np(1)O_2^+$ cation connects to O(10), O(7), O(14), O(2), and O(4) atoms from the $Np(2)O_2^+$, $Np(4)O_2^+$, and $Se(1)O_4^{2-}$ ions and two water molecules, respectively. The equatorial Np−O distances range from 2.395(4) to 2.551(4) Å. Each $Se(1)O_4^{2-}$ tetrahedron is bound to one $Np(1)O_2^+$ and one $Np(4)O_2^+$ cation, and each $Se(2)O_4^{2-}$ tetrahedron is bound to one $Np(2)O_2^+$ and one $Np(3)O_2^+$ cation in a mondentate manner. Se−O distances are in the range of 1.625(4) and 1.651(4) Å. There are eight water molecules, and every two of them bind to one NpO_2^+ cation in the equatorial plane. All water molecules point toward the interstitial space between the neptunyl selenate layers, providing hydrogen bonds linking those layers together. As discussed earlier, only the two H atoms for water O(2) atom were located in the difference maps with O−H distances of 0.82(2) and 0.83(2) Å. The bond distances between H atom and its O acceptor are 1.94(4) and 2.01(4) Å for O(12) on $Se(1)O_4^{2-}$ tetrahedron and O(8) on $Se(2)O_4^{2-}$ tetrahedron, respectively.

Table 2. Selected Interatomic Distances (Å) and Angles (deg) for $(NpO_2)_2(SeO_4)(H_2O)_4$

Np(1)−O(15)	1.852(4)	Se(1)−O(1)	1.630(5)
Np(1)−O(24)	1.841(5)	Se(1)−O(11)	1.637(4)
Np(1)−O(2)	2.458(5)	Se(1)−O(12)	1.643(4)
Np(1)−O(4)	2.474(4)	Se(1)−O(14)	1.638(5)
Np(1)−O(7)	2.407(4)	Se(2)−O(5)	1.644(4)
Np(1)−O(10)	2.398(4)	Se(2)−O(8)	1.651(4)
Np(1)−O(14)	2.444(5)	Se(2)−O(9)	1.636(4)
Np(2)−O(10)	1.843(4)	Se(2)−O(17)	1.625(4)
Np(2)−O(22)	1.852(4)	O(2)−H(1)	0.83(2)
Np(2)−O(3)	2.477(4)	O(2)−H(2)	0.82(2)
Np(2)−O(6)	2.545(4)	O(12)−H(1)	1.93(4)
Np(2)−O(16)	2.410(4)	O(8)−H(2)	2.01(4)
Np(2)−O(17)	2.401(4)	Np(1)−Np(2)	4.2103(5)
Np(2)−O(23)	2.403(4)	Np(1)−Np(4)	4.1112(5)
Np(3)−O(16)	1.846(4)	Np(1)−Np(4)	4.1908(5)
Np(3)−O(23)	1.845(4)	Np(1)−Np(4)	4.1959(5)
Np(3)−O(5)	2.447(5)	Np(2)−Np(3)	4.1320(5)
Np(3)−O(18)	2.479(4)	Np(2)−Np(3)	4.1814(5)
Np(3)−O(20)	2.481(4)	Np(2)−Np(3)	4.1837(5)
Np(3)−O(21)	2.408(4)	Np(3)−Np(4)	4.1921(5)
Np(3)−O(22)	2.395(4)	O(15)−Np(1)−O(24)	179.7(2)
Np(4)−O(7)	1.848(4)	O(10)−Np(2)−O(22)	178.5(2)
Np(4)−O(21)	1.834(4)	O(16)−Np(3)−O(23)	179.9(2)
Np(4)−O(1)	2.425(5)	O(7)−Np(4)−O(21)	178.1(2)
Np(4)−O(13)	2.551(4)		
Np(4)−O(15)	2.400(4)		
Np(4)−O(19)	2.494(4)		
Np(4)−O(24)	2.408(5)		

The cation−cation interaction (CCI) pattern in the neptunyl layers of $(NpO_2)_2(SeO_4)(H_2O)_4$ has been often found in other Np(V) compounds, such as $NpO_2Cl\cdot H_2O$[43] and $NpO_2OOCH\cdot H_2O$.[13,42] Each NpO_2^+ cation connects to four other NpO_2^+ units through CCIs to form a distorted cationic square net. For example, each $Np(1)O_2^+$ cation acts as a center coordinated by one $Np(2)O_2^+$ and one $Np(4)O_2^+$ unit and also as a ligand binds to two $Np(4)O_2^+$ centers. The Np−Np distances corresponding to CCIs range from 4.1112(5) to 4.2103(5) Å, which are comparable to other reported Np(V)−Np(V) distances corresponding to CCIs.[13] The shortest Np−Np distances perpendicular to the CCI two-dimensional network range from 7.2097(7) to 7.4332(8) Å.

$(NpO_2)_2(SeO_4)(H_2O)_2$ is isostructural with $(NpO_2)_2(SO_4)(H_2O)_2$.[24] As shown in Figure 2a, the structure of $(NpO_2)_2(SeO_4)(H_2O)_2$ is built from puckered layers of neptunyl pentagonal bipyramids in the *ab* planes, which are further connected by

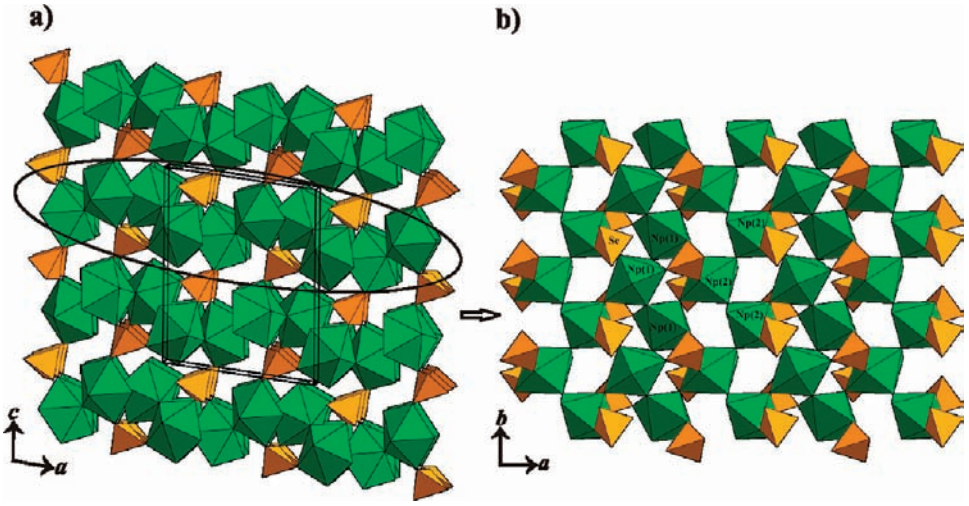

Figure 2. (a) Structure of $(NpO_2)_2(SeO_4)(H_2O)_2$ constructed by neptunyl polydedral layers (circled) that further connected by selenate anions. (b) A depiction of an individual layer of corner-sharing NpO_7 pentagonal bipyramids coordinated by SeO_4 tetrahedra.

dx.doi.org/10.1021/ic200479m |*Inorg. Chem.* 2011, 50, 5203–5214

selenate tetrahedra along the *c* axis to form a three-dimensional framework. A single neptunyl polyhedral layer is shown in Figure 2b, within which each neptunyl polyhedron shares corners with four other units and connects to one water molecule and two selenate tetrahedra above and below the plane. There are two crystallographically unique Np, one Se, and 10 O positions. The local coordination environments for Np(1) and Np(2) atoms are very similar. Both Np atoms are bonded to two O atoms in a nearly linear fashion to form NpO_2^+ cations. The Np−O distances within the NpO_2^+ unit are in the range of 1.832(4) and 1.869(4) Å, and O−Np−O angles are 177.9(2)° (Np(1)) and 178.9(2)° (Np(2)) (Table 3). Each NpO_2^+ cation is coordinated by one $Np(1)O_2^+$ unit, one $Np(2)O_2^+$ unit, two monodentate SeO_4^{2-} tetrahedra, and one water molecule in the equatorial plane to form a pentagonal bipyramid. The equatorial Np−O distances range from 2.393(4) to 2.497(4) Å. Each SeO_4^{2-} tetrahedron is bound to two $Np(1)O_2^+$ and one $Np(2)O_2^+$ cation from one neptunyl layer and one $Np(2)O_2^+$ cation from the adjacent layer. Se−O distances are in the range of 1.624(4) and 1.642(4) Å.

The CCI pattern in the neptunyl layers of $(NpO_2)_2(SeO_4)(H_2O)_2$ is very similar to that of $(NpO_2)_2(SeO_4)(H_2O)_4$. Each NpO_2^+ cation acts as a center coordinated by one $Np(1)O_2^+$ and one $Np(2)O_2^+$ unit and also as a ligand binds to one $Np(1)O_2^+$ and one $Np(2)O_2^+$ center. Therefore, each NpO_2^+ cation connects to four other NpO_2^+ units through CCIs to form a distorted cationic square net. The Np−Np distances corresponding to CCIs range from 4.1096(4) to 4.2126(4) Å, whereas the shortest Np−Np distance through a selenate anion perpendicular to the square net is 5.6378(5) Å.

$(NpO_2)_2(SeO_4)(H_2O)$ crystallizes in the monoclinic space group $P2_1/c$. The structure of $(NpO_2)_2(SeO_4)(H_2O)$ is shown in Figure 3a, which is a three-dimensional network of neptunyl pentagonal bipyramids decorated by selenate tetrahedra. Consistent with the other structures of $(NpO_2)_2(MO_4)(H_2O)_n$ (M = S, Se; n = 1, 2, 4, 6), the framework of $(NpO_2)_2(SeO_4)(H_2O)$ can be described as double chains of neptunyl polydedra along the [100] direction (Figure 3b). Each double chain connects to four identical neighbors in the *bc* plane by sharing corners between neptunyl pentagonal bipyramids, and the space between those

Table 3. Selected Interatomic Distances (Å) and Angles (deg) for $(NpO_2)_2(SeO_4)(H_2O)_2$

Np(1)−O(1)	1.869(4)	Se(1)−O(2)	1.638(4)
Np(1)−O(4)	1.832(4)	Se(1)−O(6)	1.640(4)
Np(1)−O(1)	2.439(4)	Se(1)−O(7)	1.624(4)
Np(1)−O(2)	2.497(4)	Se(1)−O(10)	1.642(4)
Np(1)−O(3)	2.466(4)	Np(1)−Np(1) × 2	4.1331(4)
Np(1)−O(5)	2.450(4)	Np(2)−Np(2) × 2	4.2126(4)
Np(1)−O(10)	2.393(4)	Np(1)−Np(2)	4.1096(4)
Np(2)−O(5)	1.846(4)	Np(1)−Np(2)	4.1282(4)
Np(2)−O(8)	1.850(4)	O(1)−Np(1)−O(4)	177.9(2)
Np(2)−O(4)	2.425(4)	O(5)−Np(2)−O(8)	178.9(2)
Np(2)−O(6)	2.440(4)		
Np(2)−O(7)	2.468(4)		
Np(2)−O(8)	2.441(4)		
Np(2)−O(9)	2.481(4)		

Table 4. Selected Interatomic Distances (Å) and Angles (deg) for $(NpO_2)_2(SeO_4)(H_2O)$

Np(1)−O(1)	1.870(4)	Se(1)−O(2)	1.628(4)
Np(1)−O(9)	1.879(4)	Se(1)−O(5)	1.622(4)
Np(1)−O(3)	2.415(4)	Se(1)−O(7)	1.626(4)
Np(1)−O(4)	2.389(4)	Se(1)−O(8)	1.655(4)
Np(1)−O(5)	2.408(4)	Np(1)−Np(2)	3.8569(4)
Np(1)−O(6)	2.361(4)	Np(1)−Np(2)	4.0276(4)
Np(1)−O(8)	2.538(4)	Np(1)−Np(2)	4.1257(4)
Np(2)−O(4)	1.854(4)	Np(1)−Np(2)	4.2262(4)
Np(2)−O(6)	1.844(4)	O(1)−Np(1)−O(9)	178.2(2)
Np(2)−O(1)	2.453(4)	O(4)−Np(2)−O(6)	177.5(2)
Np(2)−O(2)	2.370(4)	O(8)−Np(1)−O(9)	70.5(2)
Np(2)−O(7)	2.441(4)	Np(1)−O(2)	3.281(4)
Np(2)−O(8)	2.446(4)		
Np(2)−O(9)	2.486(4)		

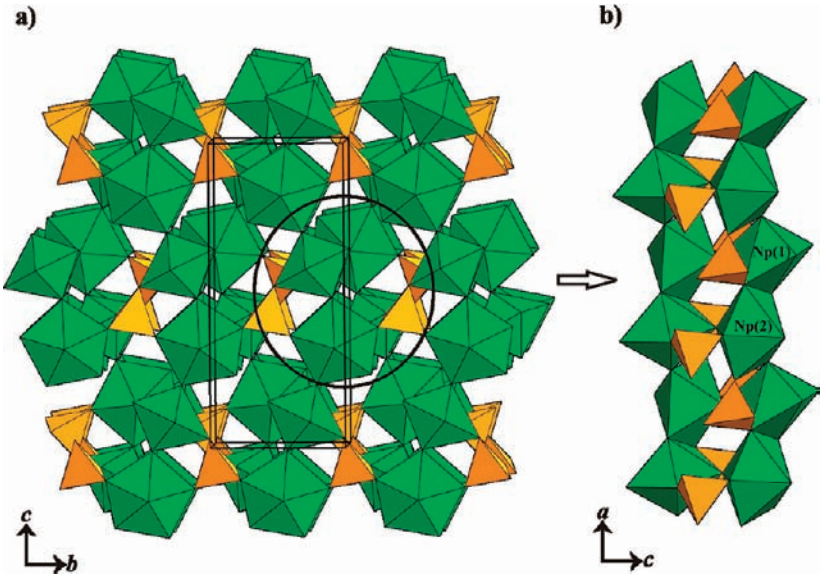

Figure 3. (a) A polyhedral presentation of the three-dimensional structure of $(NpO_2)_2(SeO_4)(H_2O)$ down the [100] direction with a double chain of neptunyl polydedra in circle. (b) A depiction of one double chain of NpO_7 pentagonal bipyramids decorated by SeO_4 tetrahedra.

dx.doi.org/10.1021/ic200479m |*Inorg. Chem.* 2011, 50, 5203–5214

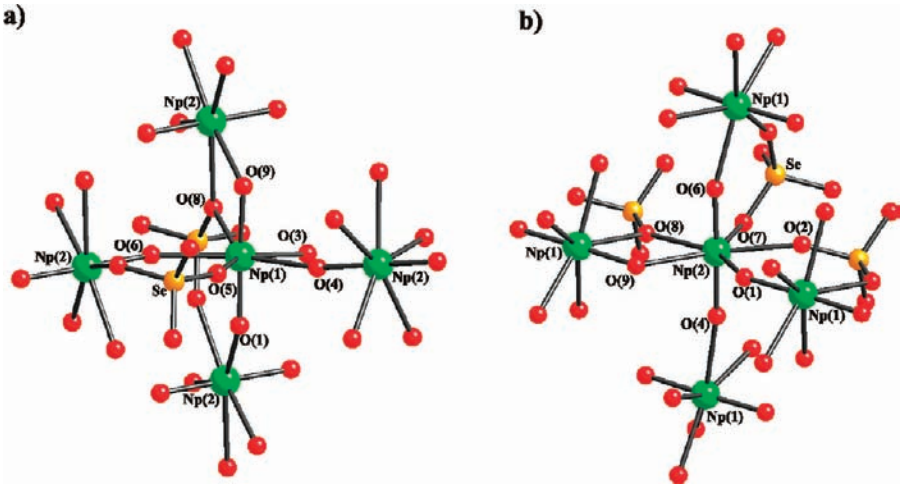

Figure 4. An illustration of the coordination environments for two Np atoms in $(NpO_2)_2(SeO_4)(H_2O)$.

chains is filled by selenate tetrahedra (Figure 3a). There are two crystallographically unique Np, one Se, and nine O positions. The local coordination environments for Np(1) and Np(2) atoms are shown in Figure 4. Each Np atom is bonded to two O atoms in a nearly linear fashion to form a NpO_2^+ cation. The Np−O distances and O−Np−O angles within the NpO_2^+ unit are 1.870(4) Å, 1.879(4) Å, and 177.5(2)° for Np(1) and 1.854(4) Å, 1.844(4) Å, and 178.2(2)° for Np(2), respectively (Table 4). Each $Np(1)O_2^+$ is coordinated by two $Np(2)O_2^+$ units (O(4), O(6)), two monodentate SeO_4^{2-} tetrahedra (O(5), O(8)), and one water molecule (O(3)) in a highly distorted pentagonal bipyramid. The equatorial Np(1)−O distances range from 2.361(4) to 2.538(4) Å, with O(8) being the longest, which is also coordinated to a $Np(2)O_2^+$ cation. O(8) atom deviates from the equatorial plane of $Np(1)O_2^+$ with a $O(8)-Np(1)-O_{np}(9)$ angle of 70.5(2)°, while other $O_{eq}-Np(1)-O_{np}(9)$ angles are close to 90° as expected (O_{np} = neptunyl oxygen, O_{eq} = equatorial oxygen). In case of Np(2), the neptunyl unit is connected to two $Np(1)O_2^+$ units (O(1), O(9)) and three monodentate SeO_4^{2-} tetrahedra (O(2), O(7), O(8)) in the equatorial plane in a pentagonal bipyramid. The $Np(2)-O_{eq}$ distances are in the range of 2.370(4) and 2.486(4) Å. Each SeO_4^{2-} tetrahedron is bound to two $Np(1)O_2^+$ and three $Np(2)O_2^+$ cations with Se−O distances between 1.622(4) and 1.655(4) Å.

The CCI pattern in $(NpO_2)_2(SeO_4)(H_2O)$ is very complex. As shown in Figure 4, each NpO_2^+ cation acts as a center coordinated by two other NpO_2^+ units and also as a ligand binds to two other NpO_2^+ centers. Therefore, each NpO_2^+ cation connects to four other NpO_2^+ units through CCIs that form a three-dimensional network of neptunyl ions. Each $Np(1)O_2^+$ and $Np(2)O_2^+$ cation also share an equatorial oxygen O(8) in addition to the CC bonds to form a dimer. Similar pairs of neptunyl have been observed in the structure of $Na_2[(NpO_2)_2(MoO_4)_2(H_2O)]\cdot H_2O$, within which they are isolated by Na^+ and MoO_4^{2-} ions and water molecules without connecting to each other.[44] The Np(1)−Np(2) distance within the edge-sharing neptunyl dimer in $(NpO_2)_2(SeO_4)(H_2O)$ is 3.8569(4) Å, which is longer than that of 3.727 Å in $Na_2[(NpO_2)_2(MoO_4)_2(H_2O)]\cdot H_2O$.[44] This results from larger Np(1)−O−Np(2) angles of 101.4(1)° and 123.6(2)° within the dimer in $(NpO_2)_2(SeO_4)(H_2O)$ caused by the deviation of O(8) from the equatorial plane of $Np(1)O_2^+$ than those of 97.2° and 114.3° in $Na_2[(NpO_2)_2(MoO_4)_2(H_2O)]\cdot H_2O$.[44] The Np(1)−Np(2) distances between two corner-sharing neptunyl polyhedra range from 4.0276(4) to 4.2262(4) Å.

The packing pattern of neptunyl polyhedra in the structure of $(NpO_2)_2(SeO_4)(H_2O)$ is very close to that of the sulfate analogue, $(NpO_2)_2(SO_4)(H_2O)$,[26] which is shown in Figure 5a. The structure of $(NpO_2)_2(SO_4)(H_2O)$ can also be divided into double chains of neptunyl polydedra decorated by sulfate tetrahedra (Figure 5b), and each double chain connects to four identical neighbors by corner-sharing. The sulfate analogue crystallizes in the orthorhombic space group *Pnma*, and Np, S, and most of the O atoms sit on special position 4c (symmetry *m*), while the corresponding atoms in the selenate deviate from the 4c position (Supporting Information), and it adopts a subgroup of *Pnma*, $P2_1/c$. The major difference between these two structures is in the coordination environment for one of the corresponding Np atoms, Np(2) atom in the sulfate and Np(1) atom in the selenate. In the structure of sulfate, the $Np(2)O_2^+$ cation is connected to four O atoms in the equatorial plane and two O(5) atoms sitting above and below the plane, which are from a single SO_4^{2-} anion. The Np(2)−O(5) distance of 2.772(8) Å is longer than usual $Np(V)-O_{eq}$ distances. As a result, each $Np(2)O_8$ polyhedron shares edges with two $Np(1)O_7$ pentagonal bipyramids along the chain direction and also shares an edge with one SO_4^{2-} tetrahedron (Figure 6a). In contrast, the corresponding O(2) and O(8) atoms in the selenate deviate from these symmetrical O(5) positions in the sulfate, and Np(1)−O distances are 3.281(4) and 2.538(4) Å for O(2) and O(8), respectively (Figure 6b). Assuming the Np(1)−O(2) distance is too long to consider any bonding interactions, the Np(1) atom in the selenate is only seven-coordinate. Each $Np(1)O_7$ polyhedron in the selenate shares an edge with one $Np(2)O_7$ pentagonal bipyramid and only shares a corner with the other one along the chain direction and with both SeO_4^{2-} tetrahedra.

Magnetism. Representative magnetic susceptibility data from powdered single crystals of $(NpO_2)_2(SeO_4)(H_2O)_4$, obtained over the temperature range of 5−320 K, are shown in Figure 7. Highlighted in the figure inset are the low temperature data showing a marked falloff in magnetization as the temperature is increased, interpreted as a ferromagnetic order of the Np moments with an onset of 8(1) K. The field response of the

dx.doi.org/10.1021/ic200479m |*Inorg. Chem.* 2011, 50, 5203–5214

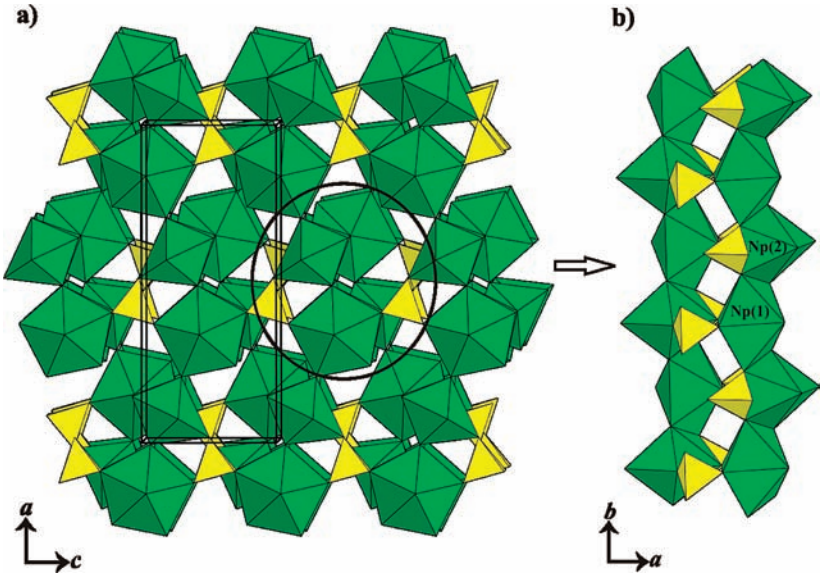

Figure 5. (a) A view of the orthorhombic $(NpO_2)_2(SO_4)(H_2O)$ structure with a double chain of green neptunyl polyhedra in circle. (b) A depiction of one double chain of NpO_8 polyhedra decorated by yellow SO_4 tetrahedra.

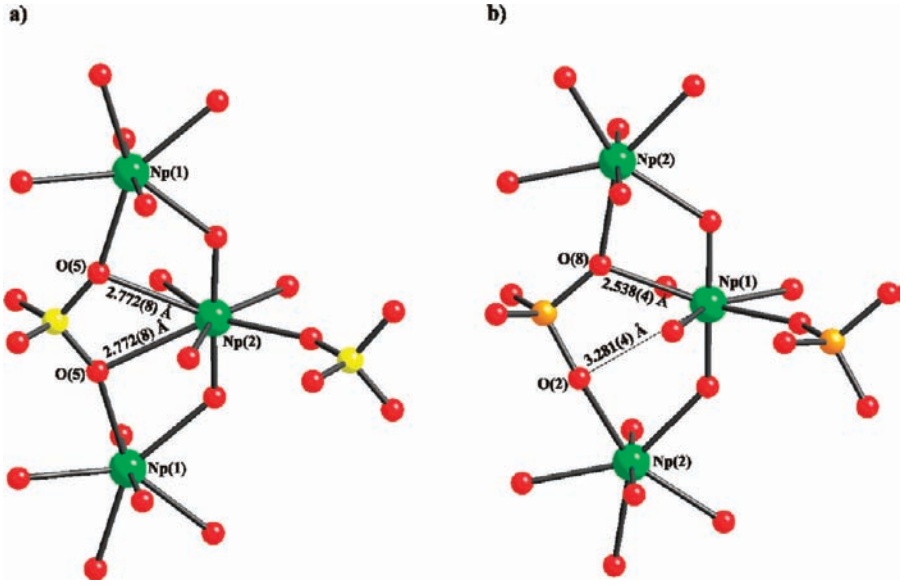

Figure 6. A comparison of the coordination environment for the Np(2) atom in $(NpO_2)_2(SO_4)(H_2O)$ (a) and the Np(1) atom in $(NpO_2)_2(SeO_4)(H_2O)$ (b).

magnetization at 2 K, shown in Figure 8, exhibits saturation behavior at low field consistent with ferromagnetic coupling at low temperatures. The saturation value of the magnetization, μ_{SAT}, represented by the high-field limit of the magnetization, is related to the ground-state wave function according to:

$$\mu_{SAT} = -gJ\mu_B$$

where J represents the total angular momentum in the Russell−Saunders formalism. The experimentally determined magnetization extrapolates to 1.98(8) μ_B, significantly less than the 3.2 μ_B expected for a full-moment f^2 system with a $^3H_4$ ground multiplet. Crystal-field splitting could reduce the moment observed here because the strong axial symmetry felt by the Np ion in the neptunyl unit reduces the free-ion spherical symmetry.[45,46] This effect requires the replacement of J states with wave functions Γ_n that include the appropriate mixing of $|m_J\rangle$ states. Crystal-field effects have been previously shown to account for similar reductions in the Pr^{3+} saturation moments in oxide systems. Pr^{3+}, which also has a f^2 configuration, has reported saturation moments ranging from negligible to about 2 μ_B or larger.[46,47] It should be noted that the attribution of a single saturation moment for Np based upon magnetization data from a powder sample may be problematic in this case because there are four crystallographically inequivalent neptunyl moieties in the structure of the tetrahydrate. However, the strong axial symmetry exerted on Np(V) by the dioxo ligation is expected to be the predominant influence on the state ordering and is the likely

dx.doi.org/10.1021/ic200479m |*Inorg. Chem.* 2011, 50, 5203–5214

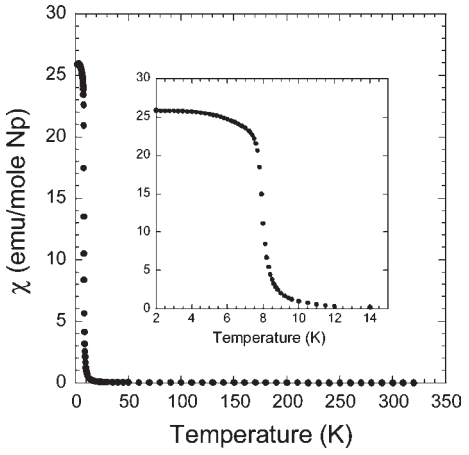

Figure 7. The magnetic susceptibility data as a function of temperature obtained from a 3.8 mg powdered sample of $(NpO_2)_2(SeO_4)(H_2O)_4$, under an applied field of 500 G. The inset focuses on the lower temperature data for the same sample, obtained under an applied field of 100 G. The shape of the magnetic response as a function of temperature is consistent with a ferromagnetic (or canted ferromagnet) ordering with a Curie temperature of 8(1) K.

cause of the reduction of the saturation moment from its free-ion value. An alternate but related explanation for the reduced saturation could arise if the ordering involves a canted-spin orientation that partially cancels the observed moment. Further single-crystal studies are required to sort out these ambiguities.

Although the moment correlations are expected to become negligible at temperatures above about twice the magnetic ordering temperature, the nonlinear M versus H curves shown in Figure 8 are evidence that they persist to temperatures as high as 20 K in $(NpO_2)_2(SeO_4)(H_2O)_4$. Persistence of correlations well above the transition temperature has been previously reported in layered materials in which in-plane coupling is stronger than any out-of-plane interactions, the latter of which may include competitive coupling forces.[48,49] The difference in Np−Np in plane distances, about 4.1−4.2 Å, from the out-of-plane shortest Np−Np interactions of 7.2−7.4 Å supports this interpretation.

Well above the temperature at which the moments appear to be ordered, the magnetic response of $(NpO_2)_2(SeO_4)(H_2O)_4$ behaves like a classic paramagnet, as described by the modified Curie Law:

$$\chi_{exp} = \frac{C}{T-\theta} + \chi_{TIP}$$

in which θ, the Weiss constant, is an indication of the an interaction energy between local spins, expressed as a temperature, and χ_{TIP} is the temperature-independent paramagnetism (TIP). C is the Curie constant and is related to the effective magnetic moment by:

$$\mu_{eff} = \left(\frac{3kC}{N{\mu_B}^2}\right)^{1/2}$$

with k as the Boltzmann constant, N as Avogadro's number, and μ_B as the Bohr magneton unit, equal to 0.927×10^{-20} erg/Gauss. A plot of χ^{-1} versus T, shown in Figure 9 over the temperature range of 50−320 K, is a straight line, which indicates that the TIP contribution is negligible and hence is not included in the fit.

Fitting the data directly to the modified Curie Law yields an effective moment of $\mu_{eff} = 3.4(2)\ \mu_B$ and a Weiss constant of

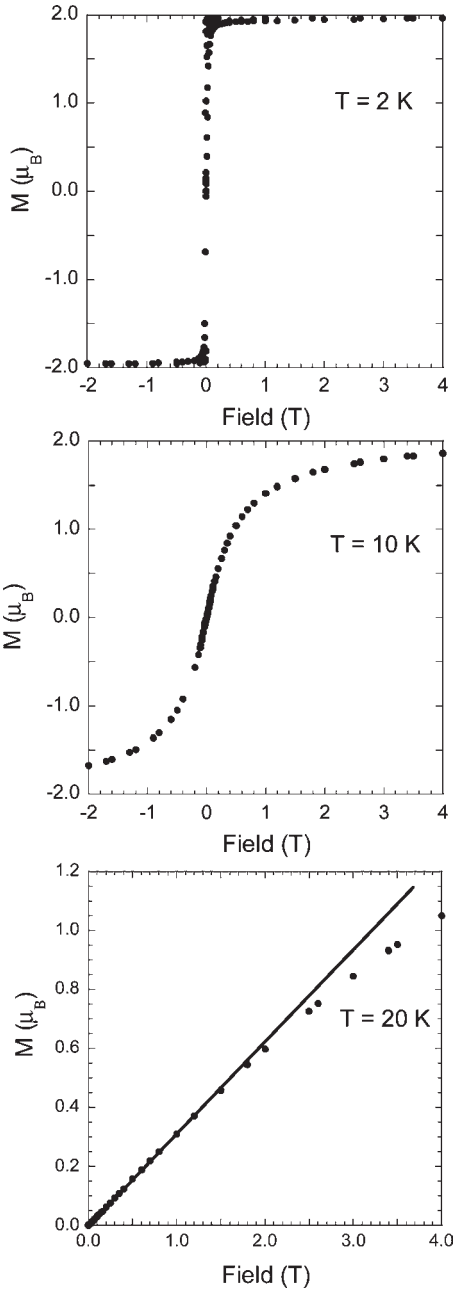

Figure 8. Magnetization as a function of fields obtained from a 3.8 mg powdered sample of $(NpO_2)_2(SeO_4)(H_2O)_4$, at 2, 10, and 20 K. The 2 K data are consistent with the response from a soft ferromagnet. The 20 K data, obtained well above the ordering temperature of 8(1) K, deviate from the straight line, included in the figure, as a function of field indicating remaining effects from ion−ion magnetic correlations, even well above T_c. The saturation moment determined from the 2 K data is 1.98(8) μ_B.

$\theta = 14(4)$ K. The effective moment is within error of the full free-ion moment 3.58 μ_B expected for an f^2 system using the Russell−Saunders coupling scheme, and the Weiss constant is small and positive, consistent with the interpretation of ferromagnetic spin ordering at 8 K.

DISCUSSION

Current studies using single-crystal X-ray diffraction show $(NpO_2)_2(SeO_4)(H_2O)_2$ and $(NpO_2)_2(SeO_4)(H_2O)_4$ to be

dx.doi.org/10.1021/ic200479m |Inorg. Chem. 2011, 50, 5203–5214

isostructural with the corresponding sulfate analogues,[24,28] whereas $(NpO_2)_2(SeO_4)(H_2O)$ is similar to, but not isostructural with, $(NpO_2)_2(SO_4)(H_2O)$.[26] These results generally agree with previous studies by Bessonov et al. who report similar CCI networks in selenate and sulfate systems.[25] However, the local connectivities between NpO_2^+ cations and MO_4^{2-} (M = S, Se) anions in $(NpO_2)_2(SeO_4)(H_2O)$ are different from those in $(NpO_2)_2(SO_4)(H_2O)$.[26] In the structure of sulfate, the SO_4^{2-} anion binds to the $Np(2)O_2^+$ cation in a bidentate manner providing two symmetrical O atoms sitting above and below the equatorial plane that result in an unusual $Np(2)O_8$ coordination geometry. In the selenate case, the corresponding two O atoms are not symmetry related; instead, they have a short and a much longer Np(1)−O distance. The SeO_4^{2-} anion binds to the $Np(1)O_2^+$ cation in a monodentate manner, and Np(1) is only seven-coordinate. The driving force for differences between these the two structures is not known in detail but may be due to the slightly different proton affinities of the SeO_4^{2-} and SO_4^{2-} anions. The trends observed here follow those previously reported for actinyl compounds containing tetrahedral oxo anions of the hexavalent group VI elements (S, Se, Cr, and Mo)[22] and the observation that uranyl to sulfate-ion orientation appears rigid in aqueous solution,[32] in contrast to uranyl selenate ion pairs, which appear to rotate freely.[33] The Np(1)−O(8)−Se angle is 118.1° in $(NpO_2)_2(SeO_4)(H_2O)$ with a monodentate linkage between neptunyl and selenate ions, and the Np(2)−O(5)−S angle is 104.2° in $(NpO_2)_2(SO_4)(H_2O)$ with a bidentate linkage. The large difference between the two angles is consistent with the two different bonding modes, although no causal relation is directly established in this work. Furthermore, both compounds adopt a condensed three-dimensional structure of NpO_2^+ cations within which tetrahedral MO_4^{2-} anions occupy the confined interstitial space. Because of its relatively larger size, the SeO_4^{2-} anion may suffer more steric constraints than the SO_4^{2-} anion within the limited space available in the neptunyl networks. A combination of these two factors may require SeO_4^{2-} anions to move away from the more symmetrical SO_4^{2-} positions. As a result, the structure of $(NpO_2)_2(SeO_4)(H_2O)$ has a lower symmetry than that of $(NpO_2)_2(SO_4)(H_2O)$, and connectivities between NpO_2^+ cations and MO_4^{2-} anions are different in the two structures.

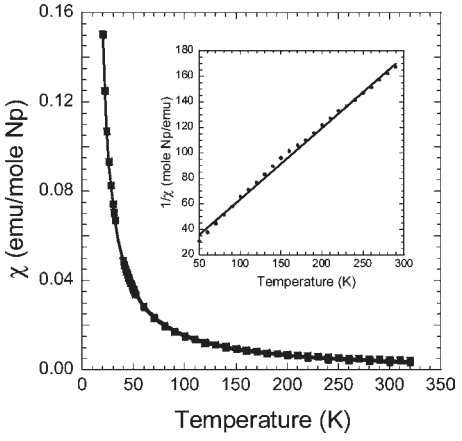

Figure 9. The magnetic susceptibility as a function of temperature above the ordering temperature. A Curie−Weiss fit to the inverse susceptibility over the temperature range of 50−300 K is shown in the inset.

On the basis of Bessonov et al.'s published studies on $(NpO_2)_2(MO_4)(H_2O)_n$ (M = S, Se; n = 1, 2, 4, 6)[25] and our current report on $(NpO_2)_2(SeO_4)(H_2O)_n$ (n = 1, 2, 4), $(NpO_2)_2(SeO_4)(H_2O)_6$ is expected to be isostructural with $(NpO_2)_2(SO_4)(H_2O)_6$.[27] If we use the structure of $(NpO_2)_2(SO_4)(H_2O)_6$ as a surrogate for $(NpO_2)_2(SeO_4)(H_2O)_6$, it is interesting to compare the structures of $(NpO_2)_2(SeO_4)(H_2O)_n$ with differing number of hydrates. As shown in Figure 10, all four structures are constructed from double chains of seven-coordinate neptunyl(V) ions linked by CCIs, which are further decorated by SeO_4^{2-} anions. In the structure of hexahydrate, one-dimensional double chains of neptunyl and selenate polyhedra are linked together by hydrogen bonds provided by water molecules. In the tetrahydrate, each double chain is connected to two other chains via CCIs to form two-dimensional layers, which are linked through hydrogen bonds provided by water molecules. Comparing the tetrahydrate structure to that of the dihydrate, the neptunyl polyhedral layers in the latter compound are more puckered and are further connected by SeO_4^{2-} anions into a three-dimensional network. Finally, each neptunyl double chain is bonded to four identical neighbors through CCIs to form a condensed three-dimensional structure in the monohydrate.

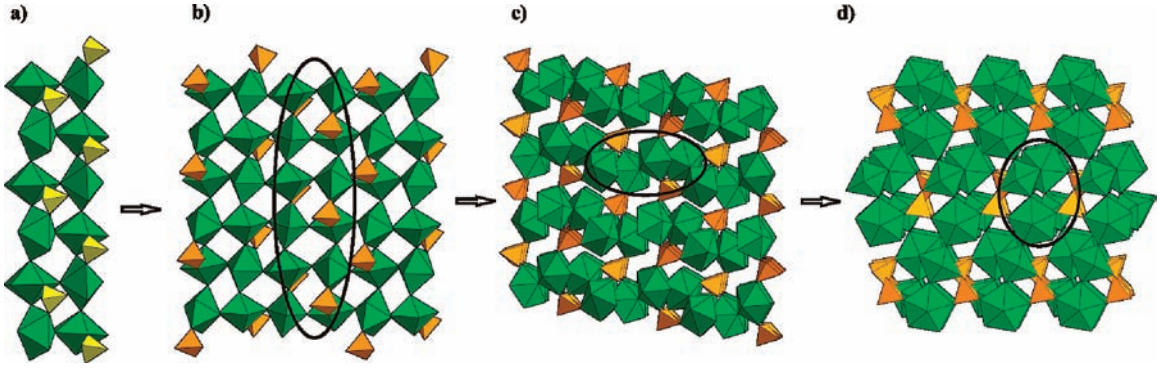

Figure 10. A structural comparison of $(NpO_2)_2(SO_4)(H_2O)_6$ and $(NpO_2)_2(SeO_4)(H_2O)_n$ (n = 1, 2, 4): (a) An individual double chain of neptunyl and sulfate polyhedra in $(NpO_2)_2(SO_4)(H_2O)_6$. (b) An individual polyhedral layer in $(NpO_2)_2(SeO_4)(H_2O)_4$ that is constructed from double chains of neptunyl and selenate polyhedra (in circle). (c) A three-dimensional structure of $(NpO_2)_2(SeO_4)(H_2O)_2$ constructed from layers of neptunyl pentagonal bipyramids that is further connected by selenate tetrahedra. A double chain of neptunyl and selenate polyhedra is in circle. (d) A three-dimensional network of neptunyl pentagonal bipyramids in $(NpO_2)_2(SeO_4)(H_2O)$ decorated by selenate tetrahedra. A double chain of neptunyl and selenate polyhedra is in circle.

dx.doi.org/10.1021/ic200479m |*Inorg. Chem.* 2011, 50, 5203–5214

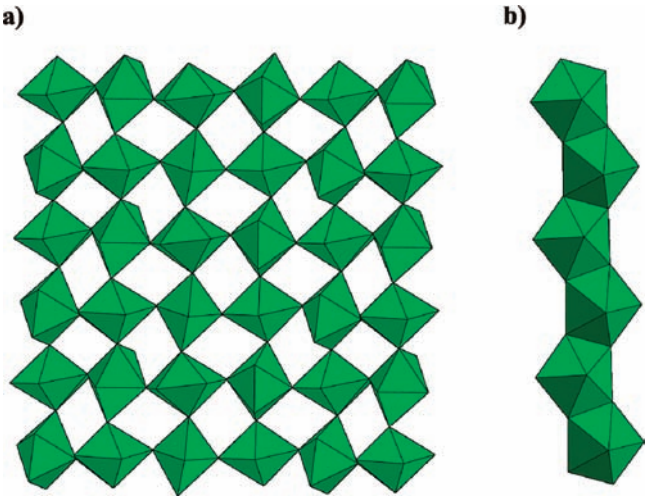

Figure 11. (a) A cationic square net of NpO_2^+ cations in ferromagnetic neptunyl(V) compounds. (b) An edge-sharing neptunyl(V) pentagonal bipyramidal chain in antiferromagnetic compounds $NaNpO_2(OH)_2$ and Np_2O_5.

The dimensionalities of the neptunyl connectivities and overall structures decrease with the number of hydrates, as reflected in the morphology of corresponding crystals. Single crystals of $(NpO_2)_2(SeO_4)(H_2O)$, $(NpO_2)_2(SeO_4)(H_2O)_2$, $(NpO_2)_2(SeO_4)(H_2O)_4$, and $(NpO_2)_2(SO_4)(H_2O)_6$[27] present in the shape of polyhedra, polyhedra, plates, and needles, respectively. In addition, the crystal shade decreases in the order of $(NpO_2)_2(SeO_4)(H_2O)$ (dark green), $(NpO_2)_2(SeO_4)(H_2O)_2$ (bright green), and $(NpO_2)_2(SeO_4)(H_2O)_4$ (pale green), consistent with relative density of Np in each structure (0.01057 Np/Å^3 for monohydrate, 0.009702 Np/Å^3 for dihydrate, and 0.007391 Np/Å^3 for tetrahydrate). The coordination environments of neptunyl cations and SeO_4^{2-} anions also gradually change with increasing hydration. In the monohydrate, each $Np(1)O_2^+$ cation is coordinated by two NpO_2^+ units, two SeO_4^{2-} tetrahedra, and one water molecule, each $Np(2)O_2^+$ cation is connected to two NpO_2^+ units and three SeO_4^{2-} tetrahedra, and each SeO_4^{2-} anion is bound to five NpO_2^+ cations. In the dihydrate structure, each NpO_2^+ cation is coordinated by two NpO_2^+ units, two SeO_4^{2-} tetrahedra, and one water molecule, and each SeO_4^{2-} tetrahedron is only bound to four NpO_2^+ cations. In the tetrahedrate, each NpO_2^+ cation is coordinated by two NpO_2^+ units, one SeO_4^{2-} tetrahedron, and two water molecules, and each SeO_4^{2-} anion is only bound to two NpO_2^+ cations. Last, in hexahydrate, one of the NpO_2^+ cations is coordinated by one NpO_2^+ and SeO_4^{2-} unit and three water molecules, the other NpO_2^+ cation is connected to two NpO_2^+ units, one SeO_4^{2-} tetrahedron, and two water molecules, and each SeO_4^{2-} anion is also only bound to two NpO_2^+ cations.

All neptunyl ions in both the sulfate and the selenate series of $(NpO_2)_2(MO_4)(H_2O)_n$ are connected to each other by CCIs. Clearly CCIs play an important role in those structures with a $Np:MO_4^{2-}$ ratio of 2:1. As stated earlier, each NpO_2^+ cation in the hexahydrate participates in three cation−cation bonds within the double chain, while in the tetrahydrate and dihydrate compounds each NpO_2^+ cation connects to four other units through CCIs to form a distorted cationic square net. In the monohydrate structure, each NpO_2^+ cation also connects to four other units via CCIs, although they form a three-dimensional neptunyl network. These compounds have been prepared under similar conditions;[24] notably $(NpO_2)_2(SeO_4)(H_2O)$, $(NpO_2)_2(SeO_4)(H_2O)_2$, and $(NpO_2)_2(SeO_4)(H_2O)_4$ crystals in the current study were obtained from the same reaction. On the basis of the stability constant determined for CCIs in acidic, aqueous solutions,[10−12] it is reasonable to assume their existence under the conditions employed herein. In fact, attempts to synthesize these materials from solutions with lower Np concentrations were unsuccessful. Similar behaviors have been found in neptunyl(V) formates, $(NpO_2)(OOCH)(H_2O)$, and $(NpO_2)(OOCH)$.[42] Both compounds were found in the same reaction, and both structures contain four CC bonds for each NpO_2^+ cation. The structure of $(NpO_2)(OOCH)(H_2O)$ consists of square cationic nets similar to those of $(NpO_2)_2(SeO_4)(H_2O)_2$ and $(NpO_2)_2(SeO_4)(H_2O)_4$, while $(NpO_2)(OOCH)$ adopts a three-dimensional diamond-like framework of NpO_2^+ cations.[42]

Details of the $(NpO_2)_2(SeO_4)(H_2O)_4$ magnetic response are consistent with a developing trend for the NpO_2^+ ion in a structure that includes CCIs. Enough magnetic studies of neptunyl(V) in several such structures have been reported that trends are beginning to emerge. For example, the observed behaviors can be divided into three simple classes depending on whether they are paramagnetic, ferromagnetic, or antiferromagnetic. There is one Np(V) compound that has been reported to behave as a simple paramagnet, $Np(NpO_2)_2(SeO_3)_3$, although there are CCIs in the structure connecting the two Np(V) sites.[50] Averaged in the susceptibility experiment with the third crystallographic Np, which is tetravalent, the effective moment/Np was found to be 2.30(5) μ_B/Np. There have also been five previous reports of CCI structures that exhibit ferromagnetism with Curie temperatures ranging from 4.5 to 12.3 K, with an average of about 7.5 K. Examples include $(NpO_2)(O_2CH)(H_2O)$,[17] $[(NpO_2)_2(O_2C)_2C_6H_4(H_2O)_3]\cdot H_2O$,[18] β-$Ag(NpO_2)(SeO_3)$,[19] $NaK_3(NpO_2)_4(SO_4)_4(H_2O)_2$,[15] and $Na(NpO_2)(SO_4)(H_2O)$.[15] The saturation moments reported from these studies are all significantly smaller than the full moment expected from an f^2 system. The results of $(NpO_2)_2(SeO_4)(H_2O)_4$ reported herein fit well into this class of behavior with an ordering temperature of 8(1) K and a saturation moment of 1.98(8) μ_B. There are two recent reports of $NaNpO_2(OH)_2$ and Np_2O_5 that comprise the third class of magnetic behavior in neptunyl(V) compounds with CCIs, antiferromagnetic ordering.[14,16] The antiferromagnetic ordering temperatures are about 20 K in these compounds, significantly higher than seen for the ferromagnetic ordering. Although the saturation moment cannot be discerned from our data, it is noted that the effective moments, determined above the ordering temperature, are significantly lower for the antiferromagnetic than for the ferromagnetic materials.

All six ferromagnetic neptunyl(V) compounds adopt low-dimensional networks of neptunyl polyhedra. More specifically, $(NpO_2)(O_2CH)(H_2O)$,[17] $[(NpO_2)_2(O_2C)_2C_6H_4(H_2O)_3]\cdot H_2O$,[18] β-$Ag(NpO_2)(SeO_3)$,[19] and $(NpO_2)_2(SeO_4)(H_2O)_4$ consist of similar two-dimensional NpO_2^+ cationic square nets as shown in Figure 11a, while $NaK_3(NpO_2)_4(SO_4)_4(H_2O)_2$ and $Na(NpO_2)(SO_4)(H_2O)$ contain four-Np wide strips of these cationic square nets.[15] Clearly, the arrangement of NpO_2^+ cations into a 2-D lattice through CCIs promotes ferromagnetic interactions between Np(V) centers. Antiferromagnetic compounds $NaNpO_2(OH)_2$ and Np_2O_5 do not exhibit cationic square nets but instead crystallize in three-dimensional frameworks of neptunyl(V) polyhedra.[14,16] Both of the latter structures are constructed by edge-sharing neptunyl(V) pentagonal bipyramidal chains as shown in Figure 11b. In the structure of $NaNpO_2(OH)_2$, these edge-sharing chains are connected to

dx.doi.org/10.1021/ic200479m |*Inorg. Chem.* 2011, 50, 5203–5214

each other through CCIs between the chains, while in Np_2O_5 chains are linked by neptunyl(V) square bipyramids into a sheet, which are further connected to each other through CCIs between the layers. On the basis of the small number of reported neptunyl(V) structures for which magnetism has been studied, it appears as though the lattice dimensionality plays an important role in the type of magnetic ordering seen at a low temperature. Presumably this correlation arises because long-range magnetic ordering is facilitated by CCIs forming superexchange pathways that interconnect these f^2 magnetic ions. What is not clear is the apparent correlation of the effective moment seen well above the critical temperature, which is dependent on the crystalline electric field and is much higher in the systems that exhibit ferromagnetism. A full analysis of optical data from selected samples is needed to relate the single ion electronic properties of Np^{5+} with the observed effective moments.

CONCLUSIONS

Single crystals of $(NpO_2)_2(SeO_4)(H_2O)_4$, $(NpO_2)_2(SeO_4)(H_2O)_2$, and $(NpO_2)_2(SeO_4)(H_2O)$ have been prepared under hydrothermal conditions, and their structures have been characterized by single-crystal X-ray diffraction. Except for the monohydrate, the results generally agree with earlier powder studies while providing much more detailed and accurate crystallographic information. $(NpO_2)_2(SeO_4)(H_2O)_4$ and $(NpO_2)_2(SeO_4)(H_2O)_2$ are isostructural with the corresponding sulfate analogues. Both structures consist of two-dimensional cationic square nets of neptunyl(V) cations, which are decorated by selenate anions. Within these nets, each NpO_2^+ cation participates in four cation−cation interactions (CCIs) with other NpO_2^+ units. In the tetrahydrate, the neptunyl and selenate layers are linked together through hydrogen bonding with water molecules, while in the dihydrate they are connected by selenate anions. The structure of $(NpO_2)_2(SeO_4)(H_2O)$ is similar to $(NpO_2)_2(SO_4)(H_2O)$,[26] but the local connectivities between one of the NpO_2^+ cations and SeO_4^{2-} anions are different from those in the sulfate, indicating a divergence between the NpO_2^+−sulfate and −selenate interactions. The structure of $(NpO_2)_2(SeO_4)(H_2O)$ adopts a three-dimensional CCI network of neptunyl(V) pentagonal bipyramids decorated by selenate tetrahedra. Each NpO_2^+ cation connects to four other NpO_2^+ units through CCIs and also shares an equatorial coordinating oxygen atom with one of other units in addition to the CC bond to form a dimer. Consistent with precedent based on the lattice connectivity of neptunyl ions, which involves in part CCIs, the tetrahydrate exhibits evidence for ferromagnetic ordering at 8(1) K.

ASSOCIATED CONTENT

Supporting Information. Crystallographic files in cif format for $(NpO_2)_2(SeO_4)(H_2O)_4$, $(NpO_2)_2(SeO_4)(H_2O)_2$, and $(NpO_2)_2(SeO_4)(H_2O)$, which are available by citing 422776 (tetrahydrate), 422777 (dihydrate), and 422778 (monohydrate) from the Inorganic Crystal Structure Database. This material is available free of charge via the Internet at http://pubs.acs.org.

AUTHOR INFORMATION

Corresponding Author

*Phone: 630-252-4364. E-mail: ls@anl.gov.

ACKNOWLEDGMENT

This work is supported by the U.S. DOE, OBES, Chemical Sciences under contract DE-AC02-06CH11357.

REFERENCES

(1) Yoshida, Z.; Johnson, S. G.; Kimura, T.; Krsul, J. R. . In *The Chemistry of the Actinide and Transactinide Elements*, 3rd ed.; Morss, L. R., Edelstein, N. M., Fuger, J., Eds.; Springer: Dordrecht, The Netherlands, 2006; Vol. 2, pp 699−812.

(2) Grenthe, I.; Drozdzynski, J.; Fujino, T.; Buck, E. C.; Albrecht-Schmitt, T. E.; Wolf, S. F. . In *The Chemistry of the Actinide and Transactinide Elements*, 3rd ed.; Morss, L. R., Edelstein, N. M., Fuger, J., Eds.; Springer: Dordrecht, 2006; Vol. 1, pp 253−698.

(3) Lieser, K. H.; Muhlenweg, U. *Radiochim. Acta* **1988**, *43*, 27–35.

(4) Silva, R. J.; Nitsche, H. *Radiochim. Acta* **1995**, *70−1*, 377–396.

(5) Kaszuba, J. P.; Runde, W. H. *Environ. Sci. Technol.* **1999**, *33*, 4427–4433.

(6) Antonio, M. R.; Soderholm, L.; Williams, C. W.; Blaudeau, J. P.; Bursten, B. E. *Radiochim. Acta* **2001**, *89*, 17–25.

(7) Burns, P. C. *Can. Mineral.* **2005**, *43*, 1839–1894.

(8) Forbes, T. Z.; Wallace, C.; Burns, P. C. *Can. Mineral.* **2008**, *46*, 1623–1645.

(9) Sullivan, J. C.; Hindman, J. C.; Zielen, A. J. *J. Am. Chem. Soc.* **1961**, *83*, 3373–3378.

(10) Guillaume, B.; Begun, G. M.; Hahn, R. L. *Inorg. Chem.* **1982**, *21*, 1159–1166.

(11) Stout, B. E.; Choppin, G. R. *Radiochim. Acta* **1993**, *61*, 65–67.

(12) Skanthakumar, S.; Antonio, M. R.; Soderholm, L. *Inorg. Chem.* **2008**, *47*, 4591–4595.

(13) Krot, N. N.; Grigoriev, M. S. *Russ. Chem. Rev.* **2004**, *73*, 89–100.

(14) Almond, P. M.; Skanthakumar, S.; Soderholm, L.; Burns, P. C. *Chem. Mater.* **2007**, *19*, 280–285.

(15) Forbes, T. Z.; Burns, P. C.; Soderholm, L.; Skanthakumar, S. *Chem. Mater.* **2006**, *18*, 1643–1649.

(16) Forbes, T. Z.; Burns, P. C.; Skanthakumar, S.; Soderholm, L. *J. Am. Chem. Soc.* **2007**, *129*, 2760–2761.

(17) Nakamoto, T.; Nakada, M.; Nakamura, A.; Haga, Y.; Onuki, Y. *Solid State Commun.* **1999**, *109*, 77–81.

(18) Nakamoto, T.; Nakada, M.; Nakamura, A. *J. Nucl. Sci. Technol.* **2002**, 102–105.

(19) Jobiliong, E.; Oshima, Y.; Brooks, J. S.; Albrecht-Schmitt, T. E. *Solid State Commun.* **2004**, *132*, 337–342.

(20) Nakamura, A.; Nakada, M.; Nakamoto, T.; Kitazawa, T.; Takeda, M. *J. Alloys Compd.* **2007**, *444*, 621–633.

(21) Forbes, T. Z.; Burns, P. C.; Soderholm, L.; Skanthakumar, S. *Mater. Res. Soc. Symp. Proc.* **2006**, *893*, 375–380.

(22) Krivovichev, S. V.; Burns, P. C. . In *Structural Chemistry of Inorganic Actinide Compounds*; Krivovichev, S. V., Burns, P. C., Tananaev, I. G., Eds.; Elsevier: Amsterdam, 2007; pp 95−182.

(23) Krivovichev, S. V. *Eur. J. Inorg. Chem.* **2010**, 2594–2603.

(24) Grigor'ev, M. S.; Ianovskii, A. I.; Fedoseev, A. M.; Budantseva, N. A.; Struchkov, I. T.; Krot, N. N.; Spitsyn, V. I. *Dokl. Akad. Nauk SSSR* **1988**, *300*, 618–622.

(25) Bessonov, A. A.; Budantseva, N. A.; Fedoseev, A. M.; Perminov, V. P.; Afonas'eva, T. V.; Krot, N. N. *Radiokhimiya* **1990**, *32*, 24–31.

(26) Grigor'ev, M. S.; Baturin, N. A.; Budantseva, N. A.; Fedoseev, A. M. *Radiokhimiya* **1993**, *35*, 29–38.

(27) Charushnikova, I. A.; Krot, N. N.; Polyakova, I. N. *Crystallogr. Rep.* **2006**, *51*, 201–204.

(28) Forbes, T. Z.; Burns, P. C. *J. Solid State Chem.* **2009**, *182*, 43–48.

(29) Forbes, T. Z.; Burns, P. C. *J. Solid State Chem.* **2005**, *178*, 3445–3452.

(30) Krivovichev, S. V.; Kahlenberg, V.; Kaindl, R.; Mersdorf, E.; Tananaev, I. G.; Myasoedov, B. F. *Angew. Chem., Int. Ed.* **2005**, *44*, 1134–1136.

(31) Krivovichev, S. V.; Kahlenberg, V.; Tananaev, I. G.; Kaindil, R.; Mersdorf, E.; Myasoedov, B. F. *J. Am. Chem. Soc.* **2005**, *127*, 1072–1073.
(32) Neuefeind, J.; Skanthakumar, S.; Soderholm, L. *Inorg. Chem.* **2004**, *43*, 2422–2426.
(33) Skanthakumar, S.; Soderholm, L. Unpublished results.
(34) Grigor'ev, M. S.; Plotnikova, T. .; Budantseva, N. A.; Fedoseev, A. M.; Yanovskii, A. I.; Struchkov, Yu. T. *Radiokhimiya* **1992**, *34*, 1–6.
(35) Rabenau, A. *Angew. Chem., Int. Ed. Engl.* **1985**, *24*, 1026–1040.
(36) Bruker. *APEX2 Version 2009.5-1 and SAINT Version 7.34a Data Collection and Processing Software*; Bruker Analytical X-Ray Instruments, Inc.: Madison, WI, 2009.
(37) Bruker. *SMART Version 5.054 Data Collection and SAINT-Plus Version 6.45a Data Processing Software for the SMART System*; Bruker Analytical X-Ray Instruments, Inc.: Madison, WI, 2003.
(38) Sheldrick, G. M. *Acta Crystallogr., Sect. A* **2008**, *64*, 112–122.
(39) Gelato, L. M.; Parthé, E. *J. Appl. Crystallogr.* **1987**, *20*, 139–143.
(40) Boudreaux, E. A.; Mulay, L. N. *Theory and Applications of Molecular Paramagnetism*; Wiley Interscience: New York, 1976.
(41) Fournier, J. M. *Structure and Bonding*; Springer Verlag: Berlin, 1985; Vols. 59−60, pp 127−196.
(42) Grigor'ev, M. S.; Yanovskii, A. I.; Struchkov, Yu. T.; Bessonov, A. A.; Afonas'eva, T. V.; Krot, N. N. *Radiokhimiya* **1993**, *34*, 1–6.
(43) Grigor'ev, M. S.; Bessonov, A. A.; Krot, N. N.; Yanovskii, A. I.; Struchkov, Yu. T. *Radiokhimiya* **1993**, *34*, 1–6.
(44) Grigor'ev, M. S.; Baturin, N. A.; Fedoseev, A. M.; Budantseva, N. A. *Koord. Khim.* **1994**, *20*, 552–556.
(45) Wybourne, B. G. *Spectrosopic Properties of Rare Earths*; Interscience: New York, 1965.
(46) Staub, U.; Soderholm, L. . In *Handbook on the Physics and Chemistry of Rare Earths*; Gschneidner, K. A., Jr., Eyring, L., Maple, M. B., Eds.; Elsevier Science BV: New York, 2000; Vol. 30, pp 491−545.
(47) Lea, K. R.; Leask, J. M.; Wolf, W. P. *J. Phys. Chem. Solids* **1962**, *23*, 1281–1405.
(48) Mason, T. E. . In *Handbook on the Physics and Chemistry of Rare Earths*; Gschneidner, K. A., Eyring, L., Maple, M. B., Eds.; Elsevier Science: New York, 2001; Vol. 31, pp 281−314.
(49) Lynn, J. W.; Skanthakumar, S. . In *Handbook on the Physics and Chemistry of Rare Earths*; Gschneidner, K. A., Eyring, L., Maple, M. B., Eds.; Elsevier Science: New York, 2001; Vol. 31, pp 315−350.
(50) Almond, P. M.; Sykora, R. E.; Skanthakumar, S.; Soderholm, L.; Albrecht-Schmitt, T. E. *Inorg. Chem.* **2004**, *43*, 958–963.